Review Article

A mathematical system of COVID-19 disease model: Existence, uniqueness, numerical and sensitivity analysis

Khadijeh Sadri [a], Hossein Aminikhah [b,c,*], Mahdi Aminikhah [d]

[a] Department of Mathematics, Near East University TRNC, Mersin 10, Nicosia, 99138, Turkey
[b] Department of Applied Mathematics and Computer Science, Faculty of Mathematical Sciences, University of Guilan, P.O. Box 1914, Rasht, 41938, Iran
[c] Center of Excellence for Mathematical Modelling, Optimization and Combinational Computing (MMOCC), University of Guilan, P.O. Box 1914, Rasht, 41938, Iran
[d] Department of Ecology and Genetics, PO Box 3000, FI-90014 University of Oulu, Finland

REVIEW HIGHLIGHTS

- We define a mathematical model to study the dynamic behaviour of COVID-19 in Iran.
- We simulate the solutions of the system using a numerical method.
- To analyze the sensitivity of the model, we propose different strategies.

ARTICLE INFO

ABSTRACT

A compartmental mathematical model of spreading COVID-19 disease in Wuhan, China is applied to investigate the pandemic behaviour in Iran. This model is a system of seven ordinary differential equations including individual behavioural reactions, governmental actions, holiday extensions, travel restrictions, hospitalizations, and quarantine. We fit the Chinese model to the Covid-19 outbreak in Iran and estimate the values of parameters by trial-error approach. We use the Adams-Bashforth predictor-corrector method based on Lagrange polynomials to solve the system of ordinary differential equations. To prove the existence and uniqueness of solutions of the model we use Banach fixed point theorem and Picard iterative method. Also, we evaluate the equilibrium points and the stability of the system. With estimating the basic reproduction number R_0, we assess the trend of new infected cases in Iran. In addition, the sensitivity analysis of the model is assessed by allocating different parameters to the system. Numerical simulations are depicted by adopting initial conditions and various values of some parameters of the system.

Specifications table

Subject area:	Mathematics and Statistics
More specific subject area:	Numerical Analysis, Biomathematics
Name of the reviewed methodology:	Finite Difference Method
Keywords:	Mathematical model; Existence and uniqueness; Adams-Bashforth predictor-corrector scheme; Equilibrium points; Stability; Basic reproduction number; Sensitivity.
Resource availability:	This method has been developed in Maple
Review question:	NA

* Corresponding author.
E-mail address: hossein.aminikhah@gmail.com (H. Aminikhah).

Method details

Mathematical modelling is a powerful tool to describe and understand precisely the nature of physical and scientific phenomena, such as models presented for the vibrational response of fluid flowing single-walled carbon nanotubes [1,2], natural and forced heat transfer in the air inside and inclined square lid-driven cavity [3], and graded nanobeam under axial and thermal loading [4]. Coronavirus disease 2019 (COVID-19) is an infectious disease that was first recognised in December 2019 in Wuhan, China, then resulted in the ongoing pandemic outbreak accompanied by millions of infections and deaths over the world. By August 8, 2020, the World Health Organization (WHO) has reported 19,187,943 confirmed cumulative cases and 716,075 deaths [5]. To understand how the virus spreads in different countries of the world, researchers of different areas have given several proposed models to analyse and predict the evolution of the pandemic, for example Lin et al. proposed a conceptual model for COVID-19 outbreak in Wuhan and considered individual behavioural reactions and governmental actions [6]. Alkahtani and Alzaid presented a mathematical model to depict the spread of the COVID-19 epidemic in Italy [7]. A compartmental mathematical model was proposed in [8] for the spread of the COVID-19 disease in Wuhan, China. Chen et al. gave a mathematical model for simulating the transmissibility of the SARS-CoV-2 in [9]. Maier and Brockmann provided a model to capture quarantine of symptomatic infected individuals and the accuracy of growing rate of observation [10]. In [11], Giordano et al. proposed a model that predicted the course of the epidemic to reach an efficient controlling strategy. Din et al. used an epidemic model for describing the dynamic of COVID-19 under convex incidence rate [12]. A fractional-order model for COVID-19 transmission was presented in [13] and its approximated solutions were obtained using the homotopy-Laplace transform method. Higazi suggested a system of fractional-order differential equations to model the COVID-19 pandemic and proved the existence of a stable solution of the model [14]. A compartmental model was proposed by Samui et al. to predict and control the transmission dynamics of the COVID-19 pandemic in India [15]. Xu et al. proposed a generalised fractional-order SEIR model denoted by SEIQRP for predicting the outbreak of COVID-19 in the USA. [16]. Ghahremanian et al. [17] prepared an overview of discovering and studying standard treatment strategies by considering RMSD, RMSF, the radius of gyration, binding free energy, and Solvent-Accessible Surface Area as effective parameters for evaluation. Wacker and Schlüter established an implicit time-discrete SIR model and applied it to available data regarding the spread of COVID-19 in Germany and Iran [18]. The first infected case in Iran was identified on February 20, 2020 [5]. The Ministry of Health and Medical Education of Iran has reported 322,567 confirmed cases and 18,132 deaths by August 8, 2020. Iran's government adopted conditions to prevent the spread of the epidemic including using masks, social differences, travel restrictions, and quarantine for four weeks that was led to a decrease of the number of individual cases and deaths until the end of April. Unfortunately, the number of daily cases and death have increased since early May and the second wave of the outbreak of the disease emerged depicted in Fig. 1.

In the current study, we try to specify the pattern of the Coronavirus in the future in Iran. Particularly, we explore whether the model can predict and control the distribution of the virus by adopting different values for some parameters of the model. We use model (1) for simulating the behaviour of COVID-19 virus in Iran. Hence, the values of parameters in the model vary and have no contradiction with conditions in Iran by trial and error. In our study, we test the numerical aspects of the presented system as well as the existence and uniqueness of the solutions of the presented model using the Banach fixed point theorem and Picard iterative method. To simulate the behaviour of state variables, an Adams-Bashforth type scheme is designed using the Lagrange polynomials and finite difference method. The estimated basic reproduction number $\mathcal{R}_0$ is used to assess the sensitivity of the model regarding some parameters of it. The main claims of the paper can be summarised as follows:

(a) Proving the existence and uniqueness of the solutions of the presented system.
(b) Constructing an Adams-Bashforth predictor-corrector method to simulate the solutions of the system.
(c) Assessing the sensitivity of the model by varying some parameters of the system.
(d) Estimating the basic reproduction number to clarify the behaviour of the virus.
(e) Simulating the behaviour of different state variables and investigating the impact of changing values of some parameters in the model.

Mathematical model of COVID-19 in Iran

In the proposed model in [6], the total population $\mathcal{N}$ is subdivided into six epidemiological compartments which lead to the following system of ordinary differential equations:

$$\begin{cases} \frac{dS(t)}{dt} = -\frac{\beta_0 F S(t)}{\mathcal{N}(t)} - \frac{\beta(t)S(t)\mathcal{I}(t)}{\mathcal{N}(t)} - \mu S(t), \\ \frac{d\mathcal{E}(t)}{dt} = \frac{\beta_0 F S(t)}{\mathcal{N}(t)} + \frac{\beta(t)S(t)\mathcal{I}(t)}{\mathcal{N}(t)} - (\sigma + \mu)\mathcal{E}(t), \\ \frac{d\mathcal{I}(t)}{dt} = \sigma\mathcal{E}(t) - (\gamma + \mu)\mathcal{I}(t), \\ \frac{d\mathcal{R}(t)}{dt} = \gamma\mathcal{I}(t) - \mu\mathcal{R}(t), \\ \frac{d\mathcal{N}(t)}{dt} = -\mu\mathcal{N}(t), \\ \frac{dD(t)}{dt} = d\gamma\mathcal{I}(t) - \lambda D(t), \\ \frac{dC(t)}{dt} = \sigma\mathcal{E}(t), \end{cases} \tag{1}$$
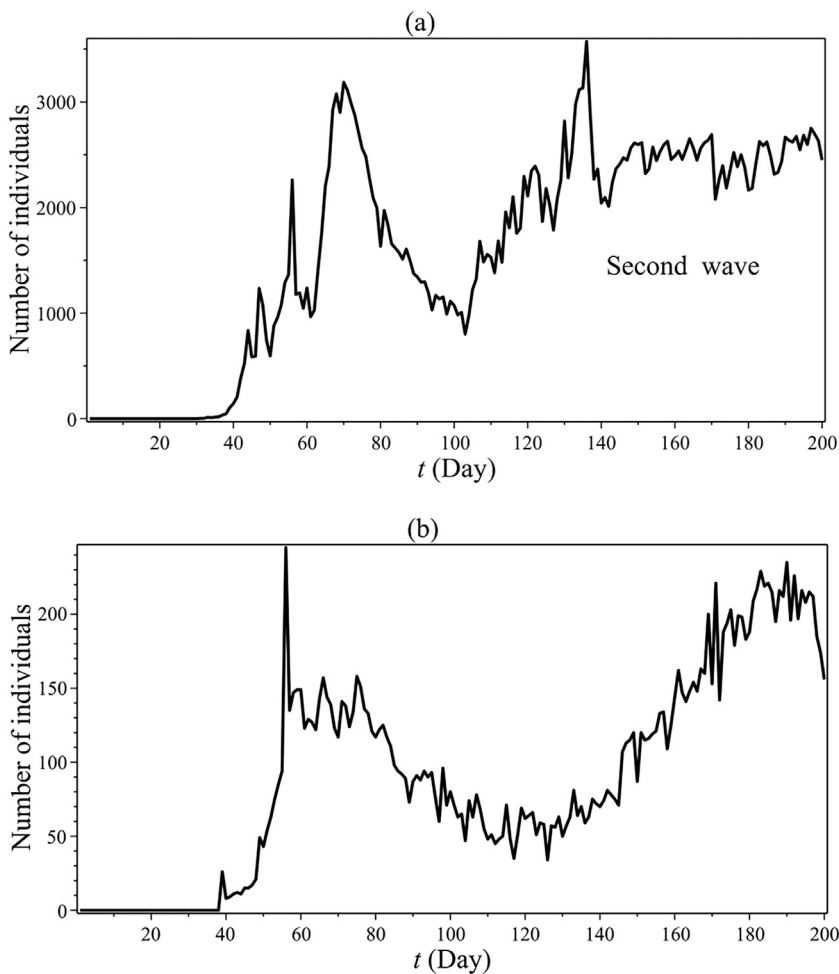
Fig. 1. The first and second waves of COVID-19 in Iran: (a) Daily confirmed cases, (b) Daily confirmed deaths.

Table 1
Values of parameters of model (1).

Notation	Parameter	Value/Range
F	Number of zoonotic cases	{10, 0}
β_0	Transmission rate	{1.2, 0.5768, 0.8}
α	Governmental action strength	{0, 0.65, 0.75}
κ	Intensity of responds	1100
μ	Emigration rate	{0.02, 0, 0.005}
σ^{-1}	Mean latent period	3
γ^{-1}	Mean infectious period	5
λ^{-1}	Mean duration of public reaction	11
d	Proportion of severe cases	0.2

where $S(t)$ represents the compartment of the susceptible population, $\mathcal{E}(t)$ represents the exposed population, $\mathcal{I}(t)$ is the infectious compartment, $\mathcal{R}(t)$ represents the removed population (recovered or dead), $\mathcal{N}(t)$ represents the total population size, $D(t)$ is the number of severe and critical cases and deaths, $C(t)$ is the number of cumulative cases (both reported and non-reported), and

$$\beta(t) = \beta_0(1 - \alpha)\left(1 - \frac{D(t)}{\mathcal{N}(t)}\right)^\kappa,$$

represents incorporating the impact of governmental action (α) and decreasing contacts amongst individuals responding to the proportion of deaths (κ). Fig. 2 shows the flowchart of the six compartments of model (1).

Parameters of model (1) and their values are described in Table 1, as seen some parameters are considered as stepwise functions due to quarantine (before, during, and after quarantine). Iran's government adopted a one-month quarantine plan from 22 March
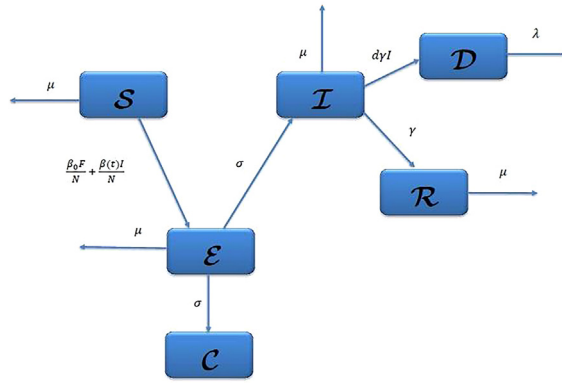
Fig. 2. Flowchart of six compartments of model (1).

to 22 April 2020 to control the virus outbreak. Hence, the governmental action strength (α), transmission rate (β_0), and emigration rate (μ) are stepwise. Values of these parameters are $\alpha = 0, \beta_0 = 1.2$, and $\mu = 0.02$ from 20 February to 21 March (before quarantine). During quarantine the values of these parameters are $\alpha = 0.65, \beta_0 = 0.5768$, and $\mu = 0$. At the end of quarantine, the values of three parameters are $\alpha = 0.75, \beta_0 = 0.8$, and $\mu = 0.005$. Note that the zoonotic transmission is not observed in Iran and only occurs the human-to-human transmission (i.e. $F = 0$).

Stability analysis

Equilibrium points

If $\mathcal{N}(t)$ and $\beta(t)$ are considered constant, that is $\mathcal{N}(t) = \mathcal{N}^*$ and $\beta(t) = \beta^*$, and since one has $\mathcal{N}(t) = S(t) + \mathcal{E}(t) + \mathcal{I}(t) + \mathcal{R}(t) + \mathcal{D}(t) + C(t)$, then the last equation in system (1) can be written as $\mathcal{E}(t) = \mathcal{N}(t) - (S(t) + \mathcal{I}(t) + \mathcal{R}(t) + \mathcal{D}(t) + C(t))$. By these assumptions, two equilibrium points P_1 and P_2 for system (1) (without the fifth equation) are computed as follows:

$$P_1 = \left(S^*, \mathcal{E}^*, \mathcal{I}^*, \mathcal{R}^*, \mathcal{D}^*, C^*\right) = \left(0, 0, 0, 0, 0, \mathcal{N}^*\right), \tag{2}$$

and

$$P_2 = \left(S^*, \mathcal{E}^*, \mathcal{I}^*, \mathcal{R}^*, \mathcal{D}^*, C^*\right) = \left(\frac{w\left(yz + \mathcal{N}^*\mu^2\right)}{\beta^*\sigma\mu}, -\frac{wz}{\beta^*\sigma}, -\frac{z}{\beta^*}, -\frac{\gamma z}{\beta^*\mu}, -\frac{d\gamma z}{\beta^*\lambda}, \frac{z(d\gamma\sigma - \lambda w) - \mathcal{N}^*\beta^*\sigma\lambda}{\beta^*\sigma\lambda}\right), \tag{3}$$

in which

$$w = \gamma + \mu, \quad y = \sigma + \mu, \quad z = \beta_0 F + \mathcal{N}^*\mu. \tag{4}$$

The Jacobian matrix of system (1) at the equilibrium points $P_i, i = 1, 2$ is as

$$\mathcal{J}\left(P_i\right) = \begin{bmatrix} -\frac{\beta_0 F + \beta^* \mathcal{I}^*}{\mathcal{N}^*} - \mu & 0 & \frac{\beta^* S^*}{\mathcal{N}^*} & 0 & 0 & 0 \\ \frac{\beta_0 F + \beta^* \mathcal{I}^*}{\mathcal{N}^*} & -y & \frac{\beta^* S^*}{\mathcal{N}^*} & 0 & 0 & 0 \\ 0 & \sigma & -w & 0 & 0 & 0 \\ 0 & 0 & \gamma & -\mu & 0 & 0 \\ 0 & 0 & d\gamma & 0 & -\lambda & 0 \\ -\sigma & 0 & -\sigma & -\sigma & -\sigma & -\sigma \end{bmatrix}. \tag{5}$$

Lemma 1. ([19]) *Suppose that $\frac{d\mathbb{W}(t)}{dt} = \mathbb{F}(t)$ is a mathematical model involving m ordinary differential equations. An equilibrium point P^* is asymptotically stable if all eigenvalues $\omega_i, i = 1, 2, \ldots, m$ corresponding to the Jacobian matrix at P^* satisfy the following condition*

$$\left|arg\left(\omega_i\right)\right| \geq \frac{\pi}{2}, \quad i = 1, 2, \ldots, m. \tag{6}$$

On the other hand, real parts of all eigenvalues must be negative.

Lemma 2 (Routh-Hurwitz conditions, [20]). *If the characteristic polynomial of the mathematical model $\frac{d\mathbb{W}(t)}{dt} = \mathbb{F}(t)$ involving m ordinary differential equations is as $f(\omega) = \omega^m + a_1\omega^{m-1} + a_2\omega^{m-2} + \cdots + a_{m-1}\omega + a_m$, then $a_m > 0$ is a necessary condition for (6).*

Now, eigenvalues of the Jacobian matrix in (5) are computed.

- Eigenvalues of the Jacobian matrix in (5) at the equilibrium point P_1 are as

$$\omega_1 = -\frac{z}{\mathcal{N}^*}, \quad \omega_2 = -y, \quad \omega_3 = -w, \quad \omega_4 = -\mu, \quad \omega_5 = -\lambda, \quad \omega_6 = -\sigma,$$

where w, y, z are defined in (4). Here, we observe that all six eigenvalues are negative values in this case. Therefore, according to Lemma 1, system (1) is asymptotically stable at the equilibrium point P_1.

- The characteristic polynomial of the Jacobian matrix in (5) at the equilibrium point P_2 is as

$$f(\omega) = \omega^6 + a_1\omega^5 + a_2\omega^4 + a_3\omega^3 + a_4\omega^2 + a_5\omega + a_6$$ where $a_6 = -wyz/\mathcal{N}^*$ is negative. By Lemma 2, system (1) is unstable at the equilibrium point P_2.

Considering the Jacobian matrix $\mathcal{J}(P_2)$ and the numerical values of the parameters in Table 1, the eigenvalues of $\mathcal{J}(P_2)$ are as follows:

$$\omega_1 = -\frac{1}{3}, \quad \omega_2 = -\frac{1}{50}, \quad \omega_3 = -\frac{1}{11}, \quad \omega_4 = -\frac{20995}{36995}, \quad \omega_5 = -\frac{18933}{345787}, \quad \omega_6 = \frac{3486}{69799},$$

which confirms $\mathcal{J}(P_2)$ has a positive eigenvalue and system (1) is unstable.

Basic reproduction number

One of the important criteria for sensitivity analysis is to investigate the following quantity:

$$\mathcal{R}_{eff} = \mathcal{R}_0 \frac{S(t)}{\mathcal{N}(t)}$$

where $\mathcal{R}_0$ is the basic reproduction number that is the spectral radius of the next generation matrix $\mathbb{F}\mathbb{V}^{-1}$, where $\mathbb{F}$ and $\mathbb{V}$ are the following Jacobian matrices

$$\mathbb{F} = \left[\frac{\partial \mathcal{F}_i(P^*)}{\partial \mathcal{X}_j}\right], \quad \mathbb{V} = \left[\frac{\partial \mathcal{V}_i(P^*)}{\partial \mathcal{X}_j}\right], \quad i, j = 1, 2,$$

and $\mathcal{F}$ and $\mathcal{V}$ are vectors constructed by the second and third equations of system (1) as follows

$$\mathcal{F} = \begin{bmatrix} \frac{\beta^* S(t)\mathcal{I}(t)}{\mathcal{N}^*} \\ 0 \end{bmatrix}, \quad \mathcal{V} = \begin{bmatrix} \frac{-\beta_0 F S(t)}{\mathcal{N}^*} + (\sigma + \mu)\mathcal{E}(t) \\ -\sigma\mathcal{E}(t) + (\gamma + \mu)\mathcal{I}(t) \end{bmatrix},$$

and $(\mathcal{X}_1, \mathcal{X}_2) = (\mathcal{E}, \mathcal{I})$. Therefore, the matrices $\mathbb{F}$ and $\mathbb{V}$ at the equilibrium P_2 are as follows

$$\mathbb{F} = \begin{bmatrix} 0 & \frac{\beta^* w(yz + \mathcal{N}^*\mu^2)}{\beta^*\sigma\mu} \\ 0 & 0 \end{bmatrix}, \mathbb{V} = \begin{bmatrix} \sigma + \mu & 0 \\ -\sigma & \gamma + \mu \end{bmatrix}.$$

So, the basic reproduction number is computed as

$$\mathcal{R}_0 = \rho\left(\mathbb{F}\mathbb{V}^{-1}\right) = \frac{(\sigma + \mu)(\beta_0 F + \mathcal{N}^*\mu) + \mathcal{N}^*\mu^2}{\mathcal{N}^*\mu(\sigma + \mu)},$$

where $\rho(\mathbb{F}\mathbb{V}^{-1})$ is the spectral radius of the generate matrix $\mathbb{F}\mathbb{V}^{-1}$. Thus, one gets

$$\mathcal{R}_{eff} = \frac{(\sigma + \mu)(\beta_0 F + \mathcal{N}^*\mu) + \mathcal{N}^*\mu^2}{\mathcal{N}^*\mu(\sigma + \mu)} \frac{S(t)}{\mathcal{N}(t)}. \tag{7}$$

The evaluated basic reproduction number for values of parameters in Table 1 is 1.0566. Because $\mathcal{R}_0 > 1$, each infected individual produces more than one new infected case and the virus can be spread through the population (more details are referred to [21]).

Existence and uniqueness of solutions of the model

In this section, the existence and uniqueness of the solutions of model (1) are proved by employing Banach fixed point theorem. First, it must be shown that the solution $(S(t), \mathcal{E}(t), \mathcal{I}(t), \mathcal{R}(t), \mathcal{N}(t), D(t), C(t))$ accompanying initial conditions $S(0) \geq 0, \mathcal{E}(0) \geq 0, \mathcal{I}(0) \geq 0, \mathcal{R}(0) \geq 0, \mathcal{N}(0) \geq 0, D(0) \geq 0, C(0) \geq 0$ are non-negative and bounded for all $t \geq 0$.

All parameters of the model are positive, thus the following equations can be considered:

$$\frac{dS(t)}{dt} = -\left(\frac{\beta_0 F}{\mathcal{N}(t)} + \frac{\beta(t)\mathcal{I}(t)}{\mathcal{N}(t)} + \mu\right)S(t) \Rightarrow \frac{dS(t)}{S(t)} = -\left(\frac{\beta_0 F}{\mathcal{N}(t)} + \frac{\beta(t)\mathcal{I}(t)}{\mathcal{N}(t)} + \mu\right)dt,$$

$$\frac{d\mathcal{E}(t)}{dt} \geq -(\sigma + \mu)\mathcal{E}(t) \Rightarrow \frac{d\mathcal{E}(t)}{\mathcal{E}(t)} \geq -(\sigma + \mu)dt,$$

$$\frac{d\mathcal{I}(t)}{dt} \geq -(\gamma + \mu)\mathcal{I}(t) \Rightarrow \frac{d\mathcal{I}(t)}{\mathcal{I}(t)} \geq -(\gamma + \mu)dt,$$

$$\frac{d\mathcal{R}(t)}{dt} \geq -\mu\mathcal{R}(t) \Rightarrow \frac{d\mathcal{R}(t)}{\mathcal{R}(t)} \geq -\mu dt,$$

$$\frac{d\mathcal{N}(t)}{dt} = -\mu\mathcal{N}(t) \Rightarrow \frac{d\mathcal{N}(t)}{\mathcal{N}(t)} = -\mu\, dt,$$

$$\frac{dD(t)}{dt} \geq -\lambda D(t) \Rightarrow \frac{dD(t)}{D(t)} \geq -\lambda\, dt,$$

$$\frac{dC(t)}{dt} = \sigma\mathcal{E}(t).$$

By solving the above equations and using the initial conditions, one has

$$S(t) = S(0)e^{-\int_0^t \left(\frac{\beta_0 F}{\mathcal{N}(\tau)} + \frac{\beta(\tau)\mathcal{I}(\tau)}{\mathcal{N}(\tau)} + \mu \right)d\tau} \geq 0,$$

$$\mathcal{E}(t) \geq \mathcal{E}(0)e^{-(\sigma+\mu)t} \geq 0,$$

$$\mathcal{I}(t) \geq \mathcal{I}(0)e^{-(\gamma+\mu)t} \geq 0,$$

$$\mathcal{R}(t) \geq \mathcal{R}(0)e^{-\mu t} \geq 0,$$

$$\mathcal{N}(t) = \mathcal{N}(0)e^{-\mu t} \geq 0,$$

$$D(t) \geq D(0)e^{-\lambda t} \geq 0,$$

$$C(t) \geq C(0) + \frac{\sigma\mathcal{E}(0)}{\sigma+\mu}\left(1 - e^{-(\sigma+\mu)t}\right) \geq 0, \quad \left(\text{if } t \to +\infty \text{ then } e^{-(\sigma+\mu)t} \to 0\right).$$

Therefore, solutions of the model along with initial conditions is non-negative for all $t \geq 0$. Since $\mathcal{N} = S + \mathcal{E} + \mathcal{I} + \mathcal{R} + D + C$, then all functions in (1) are bounded:

$$0 \leq S(t) \leq \mathcal{N}, \quad 0 \leq \mathcal{E}(t) \leq \mathcal{N}, \quad 0 \leq \mathcal{I}(t) \leq \mathcal{N},$$

$$0 \leq \mathcal{R}(t) \leq \mathcal{N}, \quad 0 \leq D(t) \leq \mathcal{N}, \quad 0 \leq C(t) \leq \mathcal{N}.$$

Now, theorems regarding the existence and uniqueness of solutions can be stated.
Let's consider the initial conditions for the system as follows:

$$\left(S(0), \mathcal{E}(0), \mathcal{I}(0), \mathcal{R}(0), \mathcal{N}(0), D(0), C(0)\right) = \left(S_0, \mathcal{E}_0, \mathcal{I}_0, \mathcal{R}_0, \mathcal{N}_0, D_0, C_0\right). \tag{8}$$

Applying the integral operator $\int_0^t (\cdot)\, dt$ to equations in model (1) leads to

$$S(t) - S(0) = \int_0^t \left(-\frac{\beta_0 F S(\tau)}{\mathcal{N}(\tau)} - \frac{\beta(\tau)S(\tau)\mathcal{I}(\tau)}{\mathcal{N}(\tau)} - \mu S(\tau) \right) d\tau,$$

$$\mathcal{E}(t) - \mathcal{E}(0) = \int_0^t \left(\frac{\beta_0 F S(\tau)}{\mathcal{N}(\tau)} + \frac{\beta(\tau)S(\tau)\mathcal{I}(\tau)}{\mathcal{N}(\tau)} - (\sigma+\mu)\mathcal{E}(\tau) \right) d\tau,$$

$$\mathcal{I}(t) - \mathcal{I}(0) = \int_0^t (\sigma\mathcal{E}(\tau) - (\gamma+\mu)\mathcal{I}(\tau))d\tau,$$

$$\mathcal{R}(t) - \mathcal{R}(0) = \int_0^t (\gamma\mathcal{I}(\tau) - \mu\mathcal{R}(\tau))d\tau,$$

$$\mathcal{N}(t) - \mathcal{N}(0) = -\int_0^t \mu\mathcal{N}(\tau)d\tau,$$

$$D(t) - D(0) = \int_0^t (d\gamma\mathcal{I}(\tau) - \lambda D(\tau))d\tau,$$

$$C(t) - C(0) = \int_0^t \sigma\mathcal{E}(\tau)d\tau = \int_0^t \sigma\left(\mathcal{N}(\tau) - (S(\tau) + \mathcal{I}(\tau) + \mathcal{R}(\tau) + D(\tau) + C(\tau))\right)d\tau. \tag{9}$$

The last equation is written based on the fact that $\mathcal{N} = S + \mathcal{E} + \mathcal{I} + \mathcal{R} + D + C$. For convenience, the following kernels are defined

$$\mathcal{K}_1(t, S) = -\frac{\beta_0 F S(t)}{\mathcal{N}(t)} - \frac{\beta(\tau)S(t)\mathcal{I}(\tau)}{\mathcal{N}(t)} - \mu S(t),$$

$$\mathcal{K}_2(t, \mathcal{E}) = \frac{\beta_0 F S(t)}{\mathcal{N}(t)} + \frac{\beta(t)S(t)\mathcal{I}(t)}{\mathcal{N}(t)} - (\sigma+\mu)\mathcal{E}(t),$$

$$\mathcal{K}_3(t, \mathcal{I}) = \sigma\mathcal{E}(t) - (\gamma+\mu)\mathcal{I}(t),$$

$$\mathcal{K}_4(t, \mathcal{R}) = \gamma\mathcal{I}(t) - \mu\mathcal{R}(t),$$

$$\mathcal{K}_5(t, \mathcal{N}) = -\mu\mathcal{N}(t),$$

$$\mathcal{K}_6(t, D) = d\gamma\mathcal{I}(t) - \lambda D(t),$$

$$\mathcal{K}_7(t, C) = \sigma\left(\mathcal{N}(t) - (S(t) + \mathcal{I}(t) + \mathcal{R}(t) + D(t) + C(t))\right).$$

Since $S, \mathcal{E}, I, \mathcal{R}, \mathcal{N}, D, C$ are non-negative bounded functions, there exist positive values $\varrho_i, i = 1, 2, \ldots, 7$ such that

$$\|S(t)\| \leq \varrho_1, \|\mathcal{E}(t)\| \leq \varrho_2, \|I(t)\| \leq \varrho_3, \|\mathcal{R}(t)\| \leq \varrho_4, \|\mathcal{N}(t)\| \leq \varrho_5, \|D(t)\| \leq \varrho_6, \|C(t)\| \leq \varrho_7.$$

Also, the following notations are considered

$$\mathcal{N}^{\dagger} = \min_{t \in [0,T]} |\mathcal{N}(t)|, \ \beta^{\dagger} = \max_{t \in [0,T]} |\beta(t)|,$$

$$\gamma_1 = \frac{\beta_0 F + \beta^{\dagger} \varrho_3}{\mathcal{N}^{\dagger}} + \mu, \gamma_2 = \sigma + \mu, \gamma_3 = \gamma + \mu, \gamma_4 = \mu, \gamma_5 = \lambda, \gamma_6 = \sigma.$$

So, Eqs. (9) can be written as follows

$$S(t) - S(0) = \int_0^t \mathcal{K}_1(\tau, S(\tau)) d\tau, \mathcal{E}(t) - \mathcal{E}(0) = \int_0^t \mathcal{K}_2(\tau, \mathcal{E}(\tau)) d\tau,$$

$$I(t) - I(0) = \int_0^t \mathcal{K}_3(\tau, I(\tau)) d\tau, \mathcal{R}(t) - \mathcal{R}(0) = \int_0^t \mathcal{K}_4(\tau, \mathcal{R}(\tau)) d\tau,$$

$$\mathcal{N}(t) - \mathcal{N}(0) = \int_0^t \mathcal{K}_5(\tau, \mathcal{N}(\tau)) d\tau, D(t) - D(0) = \int_0^t \mathcal{K}_6(\tau, D(\tau)) d\tau,$$

$$C(t) - C(0) = \int_0^t \mathcal{K}_7(\tau, C(\tau)) d\tau. \tag{10}$$

Theorem 3. If $0 \leq \Gamma = \max_{1 \leq i \leq 7} \{\gamma_i\} < 1$, then the kernels $\mathcal{K}_i, 1 \leq i \leq 7$, satisfy the Lipschitz condition and then are contradiction mappings.

Proof. Consider the kernel $\mathcal{K}_1$. Assume that $S(t)$ and $S_1(t)$ be two arbitrary functions, then one has

$$\left\|\mathcal{K}_1(t, S) - \mathcal{K}_1(t, S_1)\right\| \leq \left\|-\frac{\beta_0 F S(t)}{\mathcal{N}(t)} - \frac{\beta(t) S(t) I(t)}{\mathcal{N}(t)} - \mu S(t) + \frac{\beta_0 F S_1(t)}{\mathcal{N}(t)} + \frac{\beta(t) S_1(t) I(t)}{\mathcal{N}(t)} + \mu S_1(t)\right\|$$

$$\leq \frac{\beta_0 F}{\mathcal{N}^{\dagger}} \|S(t) - S_1(t)\| + \frac{\beta^{\dagger} \varrho_3}{\mathcal{N}^{\dagger}} \|S(t) - S_1(t)\| + \mu \|S(t) - S_1(t)\|$$

$$= \gamma_1 \|S(t) - S_1(t)\|.$$

Similar results can be obtained for kernels $\mathcal{K}_i, 2i = 2, 3, \ldots, 7$.

$$\left\|\mathcal{K}_2(t, \mathcal{E}) - \mathcal{K}_2(t, \mathcal{E}_1)\right\| \leq \left\|\frac{\beta_0 F S(t)}{\mathcal{N}(t)} + \frac{\beta(t) S(t) I(t)}{\mathcal{N}(t)} - (\sigma + \mu)\mathcal{E}(t) - \frac{\beta_0 F S(t)}{\mathcal{N}(t)} - \frac{\beta(t) S(t) I(t)}{\mathcal{N}(t)} + (\sigma + \mu)\mathcal{E}_1(t)\right\|$$

$$\leq (\sigma + \mu) \|\mathcal{E}(t) - \mathcal{E}_1(t)\|$$

$$= \gamma_2 \|\mathcal{E}(t) - \mathcal{E}_1(t)\|,$$

$$\left\|\mathcal{K}_3(t, I) - \mathcal{K}_3(t, I_1)\right\| \leq \left\|\sigma \mathcal{E}(t) - (\gamma + \mu)I(t) - \sigma \mathcal{E}(t) + (\gamma + \mu)I_1(t)\right\|$$

$$\leq (\gamma + \mu) \|I(t) - I_1(t)\| = \gamma_3 \|I(t) - I_1(t)\|,$$

$$\left\|\mathcal{K}_4(t, \mathcal{R}) - K_4(t, \mathcal{R}_1)\right\| \leq \left\|\gamma I(t) - \mu \mathcal{R}(t) - \gamma I(t) + \mu \mathcal{R}_1(t)\right\|$$

$$\leq \mu \|\mathcal{R}(t) - \mathcal{R}_1(t)\| = \gamma_4 \|\mathcal{R}(t) - \mathcal{R}_1(t)\|,$$

$$\left\|\mathcal{K}_5(t, \mathcal{N}) - \mathcal{K}_5(t, \mathcal{N}_1)\right\| \leq \left\|-\mu \mathcal{N}(t) + \mu \mathcal{N}_1(t)\right\| \leq \mu \|\mathcal{N}(t) - \mathcal{N}_1(t)\| = \gamma_4 \|\mathcal{N}(t) - \mathcal{N}_1(t)\|,$$

$$\left\|\mathcal{K}_6(t, D) - \mathcal{K}_6(t, D_1)\right\| \leq \left\|d\gamma I(t) - \lambda D(t) - d\gamma I(t) + \lambda D_1(t)\right\|$$

$$\leq \lambda \|D(t) - D_1(t)\| = \gamma_5 \|D(t) - D_1(t)\|,$$

$$\left\|\mathcal{K}_7(t, C) - \mathcal{K}_7(t, C_1)\right\| \leq \left\|\begin{array}{l} \sigma\big(\mathcal{N}(t) - (S(t) + I(t) + \mathcal{R}(t) + D(t) + C(t))\big) \\ -\sigma\big(\mathcal{N}(t) - \big(S(t) + I(t) + \mathcal{R}(t) + D(t) + C_1(t)\big)\big) \end{array}\right\|$$

$$\leq \sigma \|C(t) - C_1(t)\| = \gamma_6 \|C(t) - C_1(t)\|.$$

Therefore, the Lipschitz conditions are satisfied for $\mathcal{K}_i, i = 1, 2, \ldots, 7$. Since $0 \leq \Gamma < 1$, the kernels are contradiction mappings. $\square$

Now, using Eqs. (10), the following recursive formulas are introduced

$$S_n(t) = \int_0^t \mathcal{K}_1\big(\tau, S_{n-1}(\tau)\big)d\tau, \mathcal{E}_n(t) = \int_0^t \mathcal{K}_2\big(\tau, \mathcal{E}_{n-1}(\tau)\big)d\tau,$$

$$\mathcal{I}_n(t) = \int_0^t \mathcal{K}_3\big(\tau, \mathcal{I}_{n-1}(\tau)\big)d\tau, \mathcal{R}_n(t) = \int_0^t \mathcal{K}_4\big(\tau, \mathcal{R}_{n-1}(\tau)\big)d\tau,$$

$$\mathcal{N}_n(t) = \int_0^t \mathcal{K}_5\big(\tau, \mathcal{N}_{n-1}(\tau)\big)d\tau, D_n(t) = \int_0^t \mathcal{K}_6\big(\tau, D_{n-1}(\tau)\big)d\tau,$$

$$C_n(t) = \int_0^t \mathcal{K}_7\big(\tau, C_{n-1}(\tau)\big)d\tau.$$

Subtractions of two consecutive terms in the recursive formulas are as follow

$$\varphi_n(t) = S_n(t) - S_{n-1}(t) = \int_0^t \big(\mathcal{K}_1(\tau, S_{n-1}) - \mathcal{K}_1(\tau, S_{n-2})\big)d\tau,$$

$$\psi_n(t) = \mathcal{E}_n(t) - \mathcal{E}_{n-1}(t) = \int_0^t \big(\mathcal{K}_2(\tau, \mathcal{E}_{n-1}) - \mathcal{K}_2(\tau, \mathcal{E}_{n-2})\big)d\tau,$$

$$\xi_n(t) = \mathcal{I}_n(t) - \mathcal{I}_{n-1}(t) = \int_0^t \big(\mathcal{K}_3(\tau, \mathcal{I}_{n-1}) - \mathcal{K}_3(\tau, \mathcal{I}_{n-2})\big)d\tau,$$

$$\chi_n(t) = \mathcal{R}_n(t) - \mathcal{R}_{n-1}(t) = \int_0^t \big(\mathcal{K}_4(\tau, \mathcal{R}_{n-1}) - \mathcal{K}_4(\tau, \mathcal{R}_{n-2})\big)d\tau,$$

$$\eta_n(t) = \mathcal{N}_n(t) - \mathcal{N}_{n-1}(t) = \int_0^t \big(\mathcal{K}_5(\tau, \mathcal{N}_{n-1}) - \mathcal{K}_5(\tau, \mathcal{N}_{n-2})\big)d\tau,$$

$$\zeta_n(t) = D_n(t) - D_{n-1}(t) = \int_0^t \big(\mathcal{K}_6(\tau, D_{n-1}) - \mathcal{K}_6(\tau, D_{n-2})\big)d\tau,$$

$$\omega_n(t) = C_n(t) - C_{n-1}(t) = \int_0^t \big(\mathcal{K}_7(\tau, C_{n-1}) - \mathcal{K}_7(\tau, C_{n-2})\big)d\tau. \tag{11}$$

So, one can conclude that

$$S_n(t) = \sum_{i=1}^n \varphi_i(t), \quad \mathcal{E}_n(t) = \sum_{i=1}^n \psi_i(t), \quad \mathcal{I}_n(t) = \sum_{i=1}^n \xi_i(t), \quad \mathcal{R}_n(t) = \sum_{i=1}^n \chi_i(t),$$

$$\mathcal{N}_n(t) = \sum_{i=1}^n \eta_i(t), \quad D_n(t) = \sum_{i=1}^n \zeta_i(t), \quad C_n(t) = \sum_{i=1}^n \omega_i(t). \tag{12}$$

Now, recursive inequalities are computed for differences (11) as follows

$$\big\|\varphi_n(t)\big\| = \big\|S_n(t) - S_{n-1}(t)\big\| = \left\|\int_0^t \big(\mathcal{K}_1(\tau, S_{n-1}) - \mathcal{K}_1(\tau, S_{n-2})\big)d\tau\right\|$$

$$\leq \int_0^t \big\|\big(\mathcal{K}_1(\tau, S_{n-1}) - \mathcal{K}_1(\tau, S_{n-2})\big)\big\|d\tau,$$

$$\leq \gamma_1 t \big\|S_{n-1}(t) - S_{n-2}(t)\big\| = \gamma_1 t\big\|\varphi_{n-1}(t)\big\|,$$

$$\big\|\psi_n(t)\big\| \leq \gamma_2 t\big\|\psi_{n-1}(t)\big\|, \quad \big\|\xi_n(t)\big\| \leq \gamma_3 t\big\|\xi_{n-1}(t)\big\|, \quad \big\|\chi_n(t)\big\| \leq \gamma_4 t\big\|\chi_{n-1}(t)\big\|,$$

$$\big\|\eta_n(t)\big\| \leq \gamma_4 t\big\|\eta_{n-1}(t)\big\|, \quad \big\|\zeta_n(t)\big\| \leq \gamma_5 t\big\|\zeta_{n-1}(t)\big\|, \quad \big\|\omega_n(t)\big\| \leq \gamma_6 t\big\|\omega_{n-1}(t)\big\|. \tag{13}$$

Theorem 4. If for a time $T_0 > 0$ the following inequalities hold

$$0 < \gamma_i\, T_0 < 1, \quad i = 1, 2, \dots, 7,$$

then a unique solution exists for model (1).
Proof. The proof is divided into two parts:

(i) **Existence.** The functions in model (1) are bounded and the provided kernels satisfy the Lipschitz conditions. Therefore, the following inequalities can be obtained using (13):

$$\big\|\varphi_n\big\| \leq \gamma_1 t\, \big\|\varphi_{n-1}\big\| \leq (\gamma_1 t)^2\, \big\|\varphi_{n-2}\big\| \leq \cdots \leq \|S(0)\|\, (\gamma_1 t)^n,$$

$$\big\|\psi_n\big\| \leq \|\mathcal{E}(0)\|(\gamma_2 t)^n, \quad \big\|\xi_n\big\| \leq \|\mathcal{I}(0)\|(\gamma_3 t)^n,$$

$$\big\|\chi_n\big\| \leq \|\mathcal{R}(0)\|\, (\gamma_4 t)^n, \quad \big\|\eta_n\big\| \leq \|\mathcal{N}(0)\|(\gamma_4 t)^n,$$

$$\big\|\zeta_n\big\| \leq \|D(0)\|\, (\gamma_5 t)^n, \quad \big\|\omega_n\big\| \leq \|C(0)\|(\gamma_6 t)^n. \tag{14}$$

According to the inequalities (14), the functions defined in (12) exist and are smooth. We prove that the functions $S_n(t), \mathcal{E}_n(t), \mathcal{I}_n(t), \mathcal{R}_n(t), \mathcal{N}_n(t), D_n(t), C_n(t)$ converge to solutions of system (1). We define $\mathcal{A}_n^i(t), i = 1, 2, \ldots, 7$, as the remainder terms after n iterations, that is

$$S(t) - S(0) = S_n(t) + \mathcal{A}_n^1(t), \qquad \mathcal{E}(t) - \mathcal{E}(0) = \mathcal{E}_n(t) + \mathcal{A}_n^2(t), \qquad \mathcal{I}(t) - \mathcal{I}(0) = \mathcal{I}_n(t) + \mathcal{A}_n^3(t),$$
$$\mathcal{R}(t) - \mathcal{R}(0) = \mathcal{R}_n(t) + \mathcal{A}_n^4(t), \qquad \mathcal{N}(t) - \mathcal{N}(0) = \mathcal{N}_n(t) + \mathcal{A}_n^5(t), \qquad D(t) - D(0) = D_n(t) + \mathcal{A}_n^6(t),$$
$$C(t) - C(0) = C_n(t) + \mathcal{A}_n^7(t).$$

Using the Lipschitz condition for $\mathcal{K}_1$ leads to

$$\left\| \mathcal{A}_n^1(t) \right\| = \left\| \int_0^t \left(\mathcal{K}_1(\tau, S) - \mathcal{K}_1(\tau, S_{n-1}) \right) d\tau \right\| \leq \gamma_1 \, t \, \| S - S_{n-1} \|$$
$$\leq (\gamma_1 \, t)^2 \| S - S_{n-2} \| \leq \cdots \leq (\gamma_1 \, t)^n \left\| \mathcal{A}_0^1(t) \right\|$$
$$\leq (\gamma_1 \, t)^n \| S(t) \| \leq (\gamma_1 \, t)^n \varrho_1.$$

By setting $t = T_0$, one obtains

$$\left\| \mathcal{A}_n^1(t) \right\| \leq (\gamma_1 \, T_0)^n \varrho_1. \tag{15}$$

Taking the limit of inequality (15) as $n \to \infty$ and then using the condition $0 < \gamma_1 T_0 < 1$, one obtains $\| \mathcal{A}_n^1(t) \| \to 0$. So, $\lim_{n \to \infty} S_n(t) = S(t) - S(0)$. Similarly, the following inequalities are obtained.

$$\left\| \mathcal{A}_n^2(t) \right\| \leq (\gamma_2 \, T_0)^n \varrho_2, \qquad \left\| \mathcal{A}_n^3(t) \right\| \leq (\gamma_3 \, T_0)^n \varrho_3, \qquad \left\| \mathcal{A}_n^4(t) \right\| \leq (\gamma_4 \, T_0)^n \varrho_4,$$
$$\left\| \mathcal{A}_n^5(t) \right\| \leq (\gamma_4 \, T_0)^n \varrho_5, \qquad \left\| \mathcal{A}_n^6(t) \right\| \leq (\gamma_5 \, T_0)^n \varrho_6, \qquad \left\| \mathcal{A}_n^7(t) \right\| \leq (\gamma_6 \, T_0)^n \varrho_7. \tag{16}$$

Limiting inequalities (16) as $n \to \infty$ leads to $\| \mathcal{A}_n^i(t) \| \to 0, i = 2, 3, \ldots, 7$. Therefore, the existence of the solutions of system (1) is proved.

(ii) **Uniqueness.** Assume that $\mathcal{Y}(t)$ and $\mathcal{Y}^1(t)$ are the solution sets of model (1) such that

$$\mathcal{Y}(t) = (S(t), \mathcal{E}(t), \mathcal{I}(t), \mathcal{R}(t), \mathcal{N}(t), D(t), C(t)),$$
$$\mathcal{Y}^1(t) = (S^1(t), \mathcal{E}^1(t), \mathcal{I}^1(t), \mathcal{R}^1(t), \mathcal{N}^1(t), D^1(t), C^1(t)).$$

Then, using the condition $0 < \gamma_1 t < 1$, one has

$$\left\| S(t) - S^1(t) \right\| = \left\| \int_0^t \left(\mathcal{K}_1(\tau, S(\tau)) - \mathcal{K}_1(\tau, S^1(\tau)) \right) d\tau \right\| \leq \gamma_1 t \left\| S(t) - S^1(t) \right\|.$$

So, $(1 - \gamma_1 t) \| S(t) - S^1(t) \| \leq 0$. Finally, one gets $\| S(t) - S^1(t) \| = 0$ or $S(t) = S^1(t)$. In a similar way, one obtaines $\mathcal{E}(t) = \mathcal{E}^1(t), \mathcal{I}(t) = \mathcal{I}^1(t), \mathcal{R}(t) = \mathcal{R}^1(t), \mathcal{N}(t) = \mathcal{N}^1(t), D(t) = D^1(t), C(t) = C^1(t)$, and the uniqueness of the solutions of model (1) is proved.

Adams-Bashforth predictor-corrector scheme

In order to solve a wide variety of non-linear models, particularly models of real-world problems, many discretization methods are applied such as the Adams-Bashforth-Moulton method [22,23,24], finite difference and finite element methods [25,26]. In this paper, an Adams-Bashforth predictor-corrector scheme is described and then applied to numerical simulations of behaviour of functions in model (1) with initial conditions (8).

Consider the following system of ordinary differential equations.

$$\mathcal{X}'(t) = \mathbf{f}(t, \mathcal{X}(t)), \qquad \mathcal{X}(0) = \mathcal{X}_0, \tag{17}$$

where $\mathcal{X}(t) = (S(t), \mathcal{E}(t), \mathcal{I}(t), \mathcal{R}(t), \mathcal{N}(t), D(t), C(t))$ and $\mathcal{X}(0) = \mathcal{X}_0 = (S_0, \mathcal{E}_0, \mathcal{I}_0, \mathcal{R}_0, \mathcal{N}_0, D_0, C_0)$. Applying the integral operator $\int_0^t (\cdot) dt$ to both sides of (17), one gets

$$\mathcal{X}(t) - \mathcal{X}(0) = \int_0^t \mathbf{f}(\tau, \mathcal{X}(\tau)) \, d\tau. \tag{18}$$

Now, the time interval $[0, t]$ is discretised for step size h, so the sequence $t_{k+1} = t_k + h, k = 0, 1, \ldots, n-1, t_0 = 0, t_n = t$, is achieved. Substituting $t = t_{k+1}$ and $t = t_k$ into Eq. (18) leads to be constructed the following recursive formulas:

$$\mathcal{X}(t_{k+1}) - \mathcal{X}_0 = \int_0^{t_{k+1}} \mathbf{f}(\tau, \mathcal{X}(\tau)) \, d\tau, \tag{19}$$

$$\mathcal{X}(t_k) - \mathcal{X}_0 = \int_0^{t_k} \mathbf{f}(\tau, \mathcal{X}(\tau)) \, d\tau. \tag{20}$$
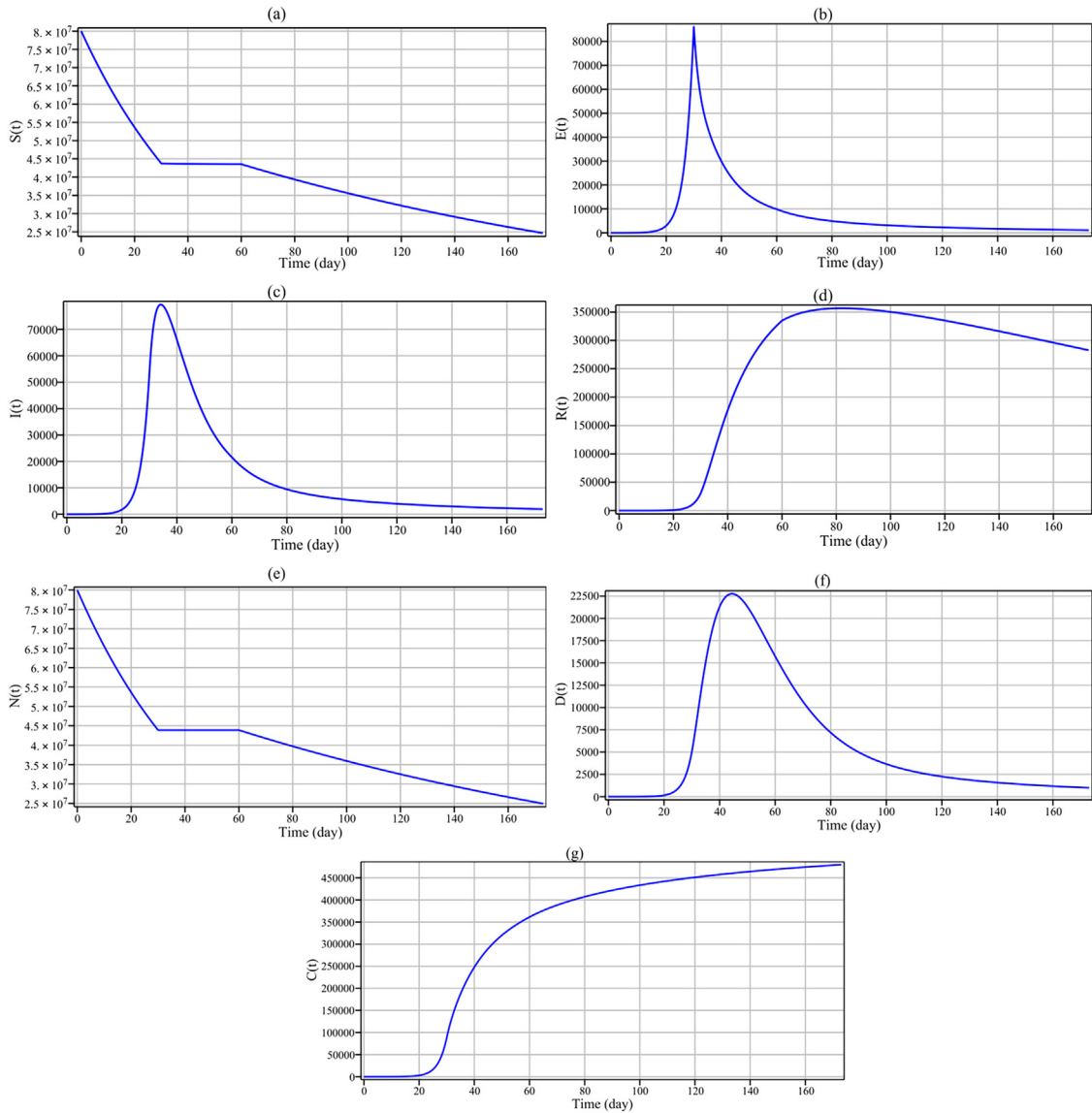
Fig. 3. Epidemic evolution predicted by the model for the COVID-19 outbreak in Iran during 173 days.

By subtracting Eq. (20) from Eq. (19) one has

$$\mathcal{X}(t_{k+1}) - \mathcal{X}(t_k) = \int_{t_k}^{t_{k+1}} \mathbf{f}(\tau, \mathcal{X}(\tau)) \, d\tau. \tag{21}$$

Now, $\mathbf{f}(\tau, \mathcal{X}(\tau))$ is approximated by the Lagrange interpolating polynomials of degree two, $\mathcal{P}_2(\tau)$, which passes through the three points $(t_{k-1}, \mathbf{f}(t_{k-1}, \mathcal{X}(t_{k-1}))), (t_k, \mathbf{f}(t_k, \mathcal{X}(t_k)))$, and $(t_{k+1}, \mathbf{f}(t_{k+1}, \mathcal{X}(t_{k+1})))$, that is

$$\mathcal{P}_2(t) = \sum_{i=0}^{2} \mathbf{f}(t_{i+k-1}, \mathcal{X}_{i+k-1}) \mathcal{L}_i(t),$$

where $\mathcal{X}_r = \mathcal{X}(t_r)$ and $\mathcal{L}_i(t)$ is the Lagrange polynomial of degree two, on the three points (t_{k-1}, t_k, t_{k+1}). Using the change of variable $s = \frac{t_{k+1} - \tau}{h}$ for Lagrange polynomials and integrating them lead to

$$
\int_{t_k}^{t_{k+1}} \mathbf{f}(\tau, \mathcal{X}(\tau)) \, d\tau \approx \int_{t_k}^{t_{k+1}} \mathcal{P}_2(\tau) \, d\tau
$$

$$
= h \int_0^1 \left[\frac{1}{2} s(1-s) \mathbf{f}(t_{k-1}, \mathcal{X}_{k-1}) + s(2-s) \mathbf{f}(t_k, \mathcal{X}_k) + \frac{1}{2}(1-s)(2-s) \mathbf{f}(t_{k+1}, \mathcal{X}_{k+1}) \right] ds
$$

$$
= \frac{h}{3} \left(2\mathbf{f}(t_k, \mathcal{X}_k) - \frac{1}{4} \mathbf{f}(t_{k-1}, \mathcal{X}_{k-1}) + \frac{5}{4} \mathbf{f}(t_{k+1}, \mathcal{X}_{k+1}) \right). \tag{22}
$$
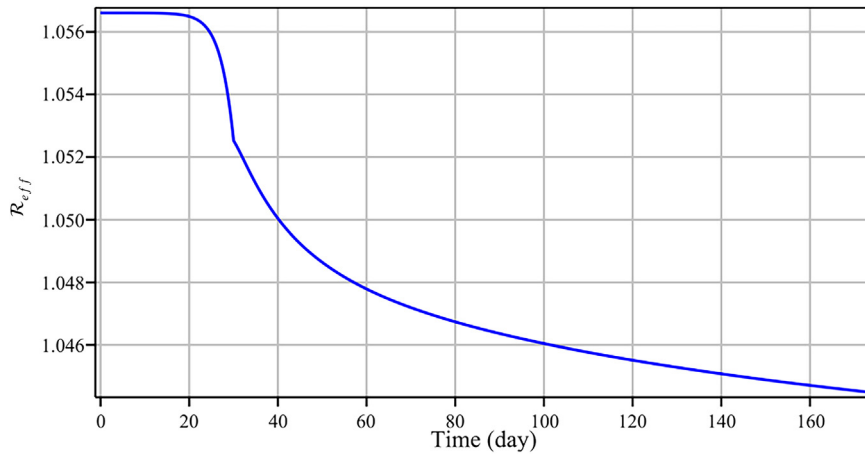
Fig. 4. Plot of the quantity $\mathcal{R}_{eff}$: Expected number of infected cases generated by one infected case.

Fig. 5. Dynamical behaviour of exposed cases (green), infected cases (red), removed and critical cases (yellow), dead population (blue), and cumulative cases (cyan) for $\alpha = 0, \mu = 0.02, \beta_0 = 1.2, \kappa = 1100$.

Therefore, the following implicit iterative formula is obtained with the aid of Eqs. (21) and (22):

$$\mathcal{X}_{k+1} = \mathcal{X}_k + \frac{h}{3}\left(2\mathbf{f}(t_k, \mathcal{X}_k) - \frac{1}{4}\mathbf{f}(t_{k-1}, \mathcal{X}_{k-1}) + \frac{5}{4}\mathbf{f}(t_{k+1}, \mathcal{X}_{k+1})\right). \tag{23}$$

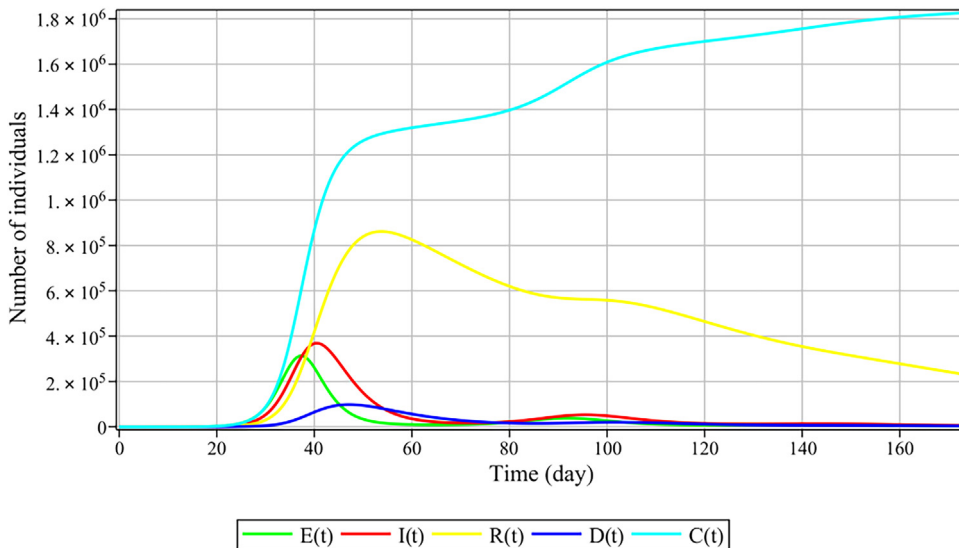For $k = 1$ we need the value of $\mathcal{X}_1 = \mathcal{X}(t_1)$ and since $\mathcal{X}_{k+1} = \mathcal{X}(t_{k+1})$ appears on both sides of Eq. (23), we need to predict the values of $\mathcal{X}(t_{k+1})$ and $\mathcal{X}(t_1)$ on the right-hand side of Eq. (23). Hence, the following predictor-corrector scheme is proposed:

$$\begin{cases} \mathcal{X}_1^P = \mathcal{X}_0 + h\,\mathbf{f}(t_0, \mathcal{X}_0), \\ \mathcal{X}_1 = \mathcal{X}_0 + \frac{h}{2}\left(\mathbf{f}(t_0, \mathcal{X}_0) + \mathbf{f}(t_1, \mathcal{X}_1^P)\right), \end{cases}$$
$$\begin{cases} \mathcal{X}_{k+1}^P = \mathcal{X}_k + h\,\mathbf{f}(t_k, \mathcal{X}_k), \\ \mathcal{X}_{k+1} = \mathcal{X}_k + \frac{h}{3}\left(2\mathbf{f}(t_k, \mathcal{X}_k) - \frac{1}{4}\mathbf{f}(t_{k-1}, \mathcal{X}_{k-1}) + \frac{5}{4}\mathbf{f}(t_{k+1}, \mathcal{X}_{k+1}^P)\right), \\ \quad k = 1, 2, \ldots, . \end{cases} \tag{24}$$
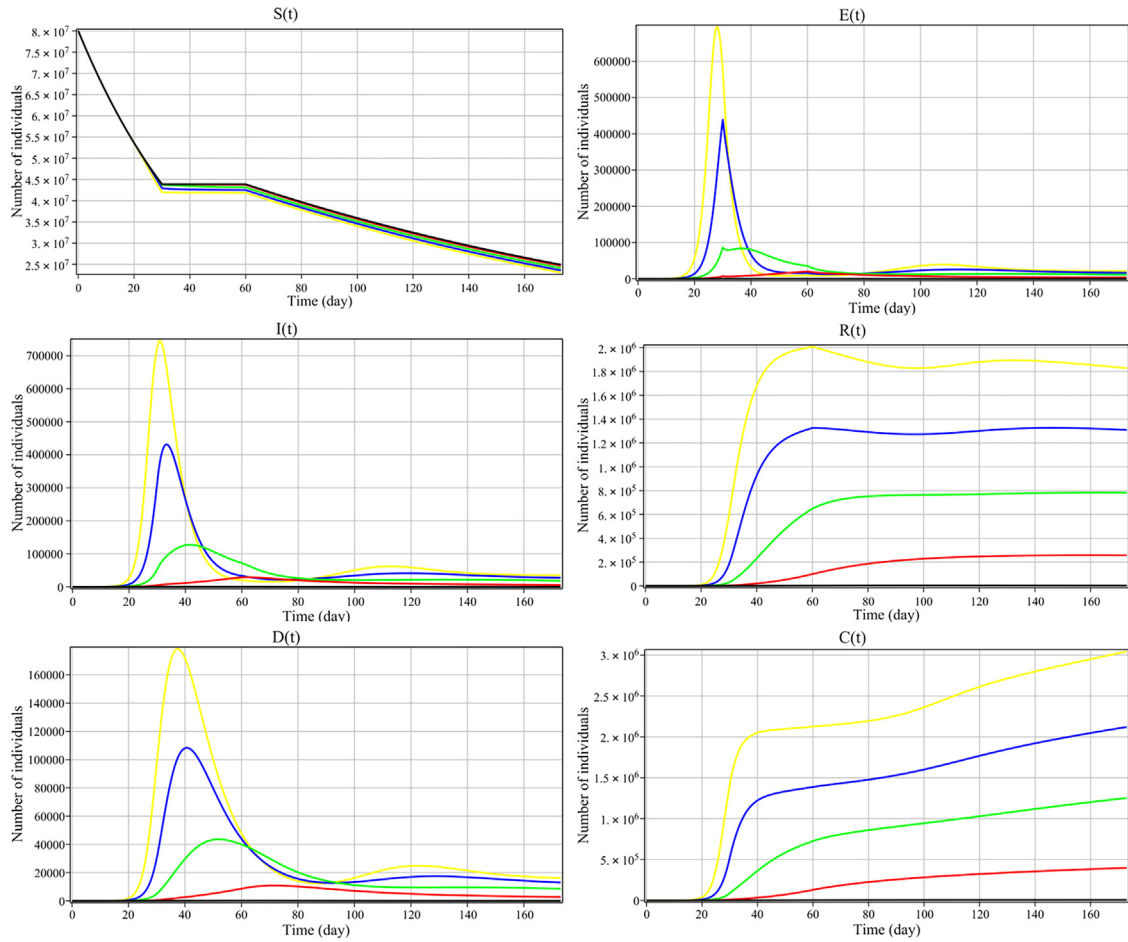
Fig. 6. Sensitivity analysis of the model regarding β_0 for: $\beta_0 = 0.6$ (black solid), $\beta_0 = 0.9$ (red solid), $\beta_0 = 1.2$ (green solid), $\beta_0 = 1.5$ (blue solid), $\beta_0 = 1.8$ (yellow solid).

So, the approximate solutions of model (1) are as follows:

$$
\begin{cases}
S_1^P = S_0 - h\left(\frac{\beta_0 F S_0}{\mathcal{N}_0} + \frac{\beta(t)S_0 \mathcal{I}_0}{\mathcal{N}_0} + \mu S_0\right), \\
\mathcal{E}_1^P = \mathcal{E}_0 + h\left(\frac{\beta_0 F S_0}{\mathcal{N}_0} + \frac{\beta(t)S_0 \mathcal{I}_0}{\mathcal{N}_0} - (\sigma + \mu)S_0\right), \\
\mathcal{I}_1^P = \mathcal{I}_0 + h\left(\sigma \mathcal{E}_0 - (\gamma + \mu)\mathcal{I}_0\right), \\
\mathcal{R}_1^P = \mathcal{R}_0 + h\left(\gamma \mathcal{I}_0 - \mu \mathcal{R}_0\right), \\
\mathcal{N}_1^P = \mathcal{N}_0 - h\mu \mathcal{N}_0, \\
\mathcal{D}_1^P = \mathcal{D}_0 + h\left(d\gamma \mathcal{I}_0 - \lambda \mathcal{D}_0\right), \\
\mathcal{C}_1^P = \mathcal{C}_0 + h\sigma \mathcal{E}_0,
\end{cases}
$$

$$
\begin{cases}
S_1 = S_0 - \frac{h}{2}\left(\frac{\beta_0 F S_0}{\mathcal{N}_0} + \frac{\beta(t)S_0 \mathcal{I}_0}{\mathcal{N}_0} + \mu S_0 + \frac{\beta_0 F S_1^P}{\mathcal{N}_1^P} + \frac{\beta(t)S_1^P \mathcal{I}_1^P}{\mathcal{N}_1^P} + \mu S_1^P\right), \\
\mathcal{E}_1 = \mathcal{E}_0 + \frac{h}{2}\left(\frac{\beta_0 F S_0}{\mathcal{N}_0} + \frac{\beta(t)S_0 \mathcal{I}_0}{\mathcal{N}_0} - (\sigma + \mu)S_0 + \frac{\beta_0 F S_1^P}{\mathcal{N}_1^P} + \frac{\beta(t)S_1^P \mathcal{I}_1^P}{\mathcal{N}_1^P} - (\sigma + \mu)S_1^P\right), \\
\mathcal{I}_1 = \mathcal{I}_0 + \frac{h}{2}\left(\sigma \mathcal{E}_0 - (\gamma + \mu)\mathcal{I}_0 + \sigma \mathcal{E}_1^P - (\gamma + \mu)\mathcal{I}_1^P\right), \\
\mathcal{R}_1 = \mathcal{R}_0 + \frac{h}{2}\left(\gamma \mathcal{I}_0 - \mu \mathcal{R}_0 + \gamma \mathcal{I}_1^P - \mu \mathcal{R}_1^P\right), \\
\mathcal{N}_1 = \mathcal{N}_0 - \frac{h}{2}\left(\mu \mathcal{N}_0 + \mu \mathcal{N}_1^P\right), \\
\mathcal{D}_1 = \mathcal{D}_0 + \frac{h}{2}\left(d\gamma \mathcal{I}_0 - \lambda \mathcal{D}_0 + d\gamma \mathcal{I}_1^P - \lambda \mathcal{D}_1^P\right), \\
\mathcal{C}_1 = \mathcal{C}_0 + \frac{h}{2}\left(\sigma \mathcal{E}_0 + \sigma \mathcal{E}_1^P\right),
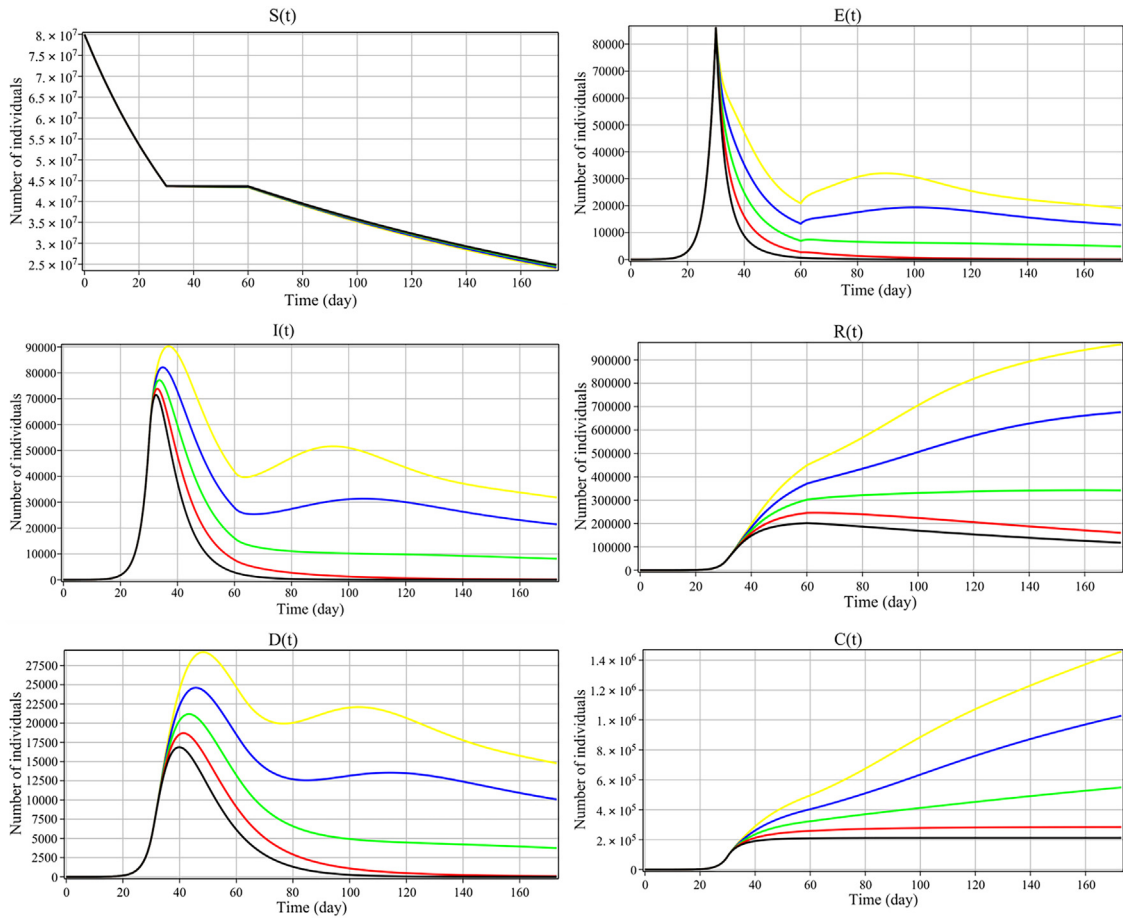\end{cases}
$$

Fig. 7. Sensitivity analysis of the model regarding α while $\alpha = 0.5$ (yellow solid), $\alpha = 0.6$ (blue solid), $\alpha = 0.7$ (green solid), $\alpha = 0.8$ (red solid), $\alpha = 0.9$ (black solid).

$$
\begin{cases}
S_{k+1}^P = S_k - h\left(\frac{\beta_0 F S_k}{\mathcal{N}_k} + \frac{\beta(t) S_k \mathcal{I}_k}{\mathcal{N}_k} + \mu S_k\right), \\[4pt]
\mathcal{E}_{k+1}^P = \mathcal{E}_k + h\left(\frac{\beta_0 F S_k}{\mathcal{N}_k} + \frac{\beta(t) S_k \mathcal{I}_k}{\mathcal{N}_k} - (\sigma + \mu) S_k\right), \\[4pt]
\mathcal{I}_{k+1}^P = \mathcal{I}_k + h\left(\sigma \mathcal{E}_k - (\gamma + \mu)\mathcal{I}_k\right), \\[4pt]
\mathcal{R}_{k+1}^P = \mathcal{R}_k + h\left(\gamma \mathcal{I}_k - \mu \mathcal{R}_k\right), \\[4pt]
\mathcal{N}_{k+1}^P = \mathcal{N}_k - h\mu \mathcal{N}_k, \\[4pt]
\mathcal{D}_{k+1}^P = \mathcal{D}_k + h\left(d\gamma \mathcal{I}_k - \lambda \mathcal{D}_k\right), \\[4pt]
C_{k+1}^P = C_k + h\sigma \mathcal{E}_k,
\end{cases}
$$

$$
\begin{cases}
S_{k+1} = S_k + \frac{h}{3}\left(\begin{aligned}&\tfrac{1}{4}\left(\frac{\beta_0 F S_{k-1}}{\mathcal{N}_{k-1}} + \frac{\beta(t) S_{k-1}\mathcal{I}_{k-1}}{\mathcal{N}_{k-1}} + \mu S_{k-1}\right) - 2\left(\frac{\beta_0 F S_k}{\mathcal{N}_k} + \frac{\beta(t) S_k \mathcal{I}_k}{\mathcal{N}_k} + \mu S_k\right) \\ &-\tfrac{5}{4}\left(\frac{\beta_0 F S_{k+1}^P}{\mathcal{N}_{k+1}^P} + \frac{\beta(t) S_{k+1}^P \mathcal{I}_{k+1}^P}{\mathcal{N}_{k+1}^P} + \mu S_{k+1}^P\right)\end{aligned}\right), \\[10pt]
\mathcal{E}_{k+1} = \mathcal{E}_k + \frac{h}{3}\left(\begin{aligned}&2\left(\frac{\beta_0 F S_k}{\mathcal{N}_k} + \frac{\beta(t) S_k \mathcal{I}_k}{\mathcal{N}_k} - (\sigma+\mu)S_k\right) - \tfrac{1}{4}\left(\frac{\beta_0 F S_{k-1}}{\mathcal{N}_{k-1}} + \frac{\beta(t) S_{k-1}\mathcal{I}_{k-1}}{\mathcal{N}_{k-1}} - (\sigma+\mu)S_{k-1}\right) \\ &+\tfrac{5}{4}\left(\frac{\beta_0 F S_{k+1}^P}{\mathcal{N}_{k+1}^P} + \frac{\beta(t) S_{k+1}^P \mathcal{I}_{k+1}^P}{\mathcal{N}_{k+1}^P} - (\sigma+\mu)S_{k+1}^P\right)\end{aligned}\right), \\[10pt]
\mathcal{I}_{k+1} = \mathcal{I}_k + \frac{h}{3}\left(2\left(\sigma\mathcal{E}_k - (\gamma+\mu)\mathcal{I}_k\right) + \tfrac{1}{4}\left(\sigma\mathcal{E}_{k-1} - (\gamma+\mu)\mathcal{I}_{k-1}\right) + \tfrac{5}{4}\left(\sigma\mathcal{E}_{k+1}^P - (\gamma+\mu)\mathcal{I}_{K+1}^P\right)\right), \\[6pt]
\mathcal{R}_{k+1} = \mathcal{R}_k + \frac{h}{3}\left(2\left(\gamma\mathcal{I}_k - \mu\mathcal{R}_k\right) - \tfrac{1}{4}\left(\gamma\mathcal{I}_{k-1} - \mu\mathcal{R}_{k-1}\right) + \tfrac{5}{4}\left(\gamma\mathcal{I}_{k+1}^P - \mu\mathcal{R}_{k+1}^P\right)\right), \\[6pt]
\mathcal{N}_{k+1} = \mathcal{N}_k + \frac{h}{3}\left(\tfrac{1}{4}\mu\mathcal{N}_{k-1} - 2\mu\mathcal{N}_k - \tfrac{5}{4}\mu\mathcal{N}_{k+1}^P\right), \\[6pt]
\mathcal{D}_{k+1} = \mathcal{D}_k + \frac{h}{3}\left(2\left(d\gamma\mathcal{I}_k - \lambda\mathcal{D}_k\right) - \tfrac{1}{4}\left(d\gamma\mathcal{I}_{k-1} - \lambda\mathcal{D}_{k-1}\right) + \tfrac{5}{4}\left(d\gamma\mathcal{I}_{k+1}^P - \lambda\mathcal{D}_{k+1}^P\right)\right), \\[6pt]
C_{k+1} = C_k + \frac{h}{3}\left(2\sigma\mathcal{E}_k - \tfrac{1}{4}\sigma\mathcal{E}_{k-1} + \tfrac{5}{4}\sigma\mathcal{E}_{k+1}^P\right),
\end{cases}
$$

Table 2
Values of stepwise parameters before, during, and after quarantine in Iran.

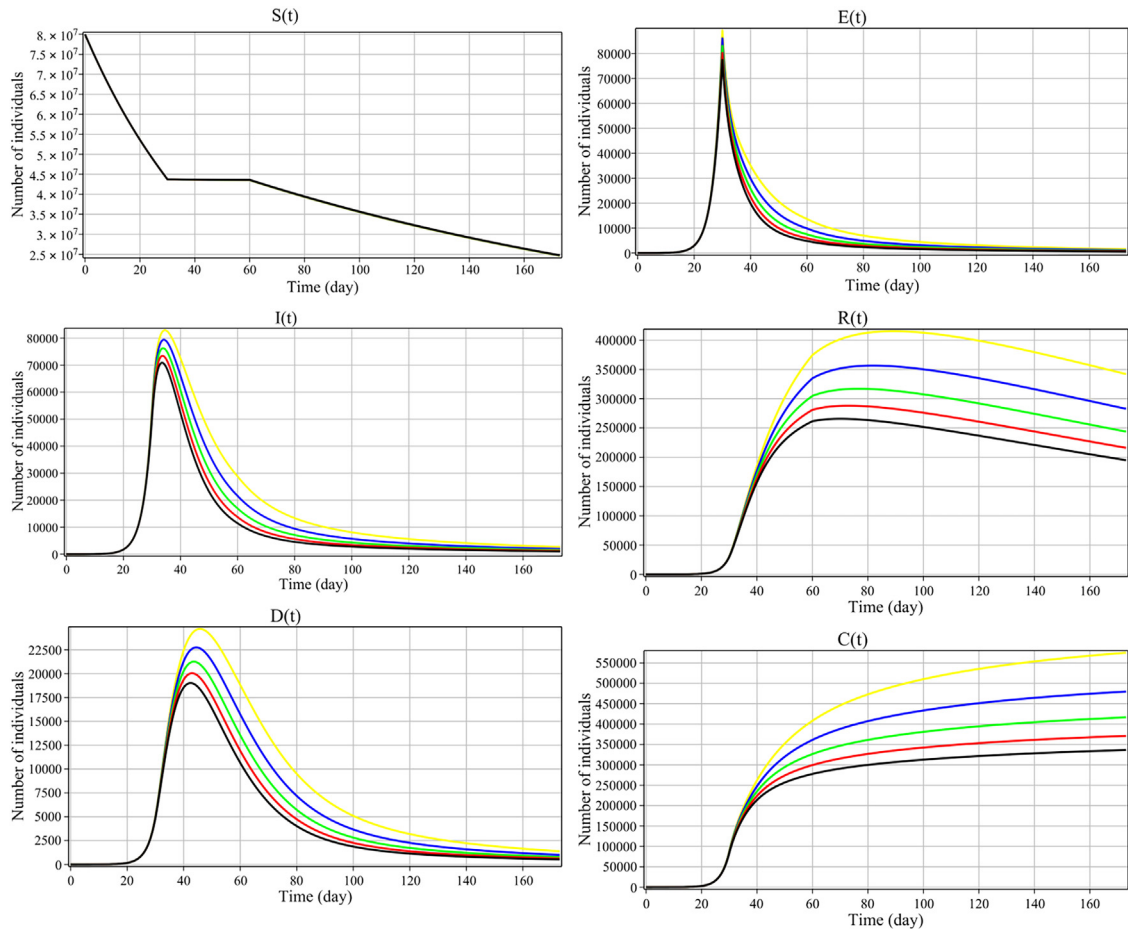| Parameter	20 February-21 March	22 March-22 April	After 22 April
α	0	0.65	0.75
β_0	1.2	0.5768	0.8
μ	0.02	0	0.005

Fig. 8. Sensitivity analysis of the model regarding κ while $\kappa = 800$ (yellow solid), $\kappa = 1100$ (blue solid), $\kappa = 1400$ (green solid), $\kappa = 1700$ (red solid), $\kappa = 2000$ (black solid).

Numerical simulations

In this section, the numerical simulations are presented. The date of first two confirmed cases, 20 February 2020, is considered as the beginning of the simulation. Iran's government announced quarantine conditions from 22 March for four weeks. Because of this reason, the parameters α, β_0, and μ are assumed as stepwise functions and their values are selected based on Table 2.

The initial conditions are selected as follows:

$$\mathcal{N}(0) = 80 \times 10^6, \quad \mathcal{S}(0) = \mathcal{N}(0) - 6, \quad \mathcal{E}(0) = 2, \quad \mathcal{I}(0) = 2, \quad \mathcal{R}(0) = 0, \quad \mathcal{D}(0) = 0, \quad \mathcal{C}(0) = 2.$$

According to the report of the Ministry of Health and Medical Education of Iran, the total of confirmed cases, dead, recovered, severe, and critical cases are 322,567, 18,132, 282,122, and 4148, respectively, by 8 August 2020. Parts of (a)-(g) of Fig. 3 show the behaviour of all variables $\mathcal{S}(t), \mathcal{E}(t), \mathcal{I}(t), \mathcal{R}(t), \mathcal{N}(t), \mathcal{D}(t)$, and $\mathcal{C}(t)$ of model (1) in a 173-day time interval (20 Feb-8 Aug) for $T = 173, h = 0.01$, and $\kappa = 1100$. The number of exposed people and infected people ($\mathcal{E}(t)$ and $\mathcal{I}(t)$) increases before quarantine, but after carrying out quarantine, the number of people in these two compartments is controlled significantly and have a decreasing treatment (Fig. 3). In the first thirty days of the appearance of the disease, the number of recovered or dead persons, $\mathcal{R}(t)$, increase by negligible amount. Then it reaches a sharp increase until to eighty days. For the last 100 days it decreases gradually. The number
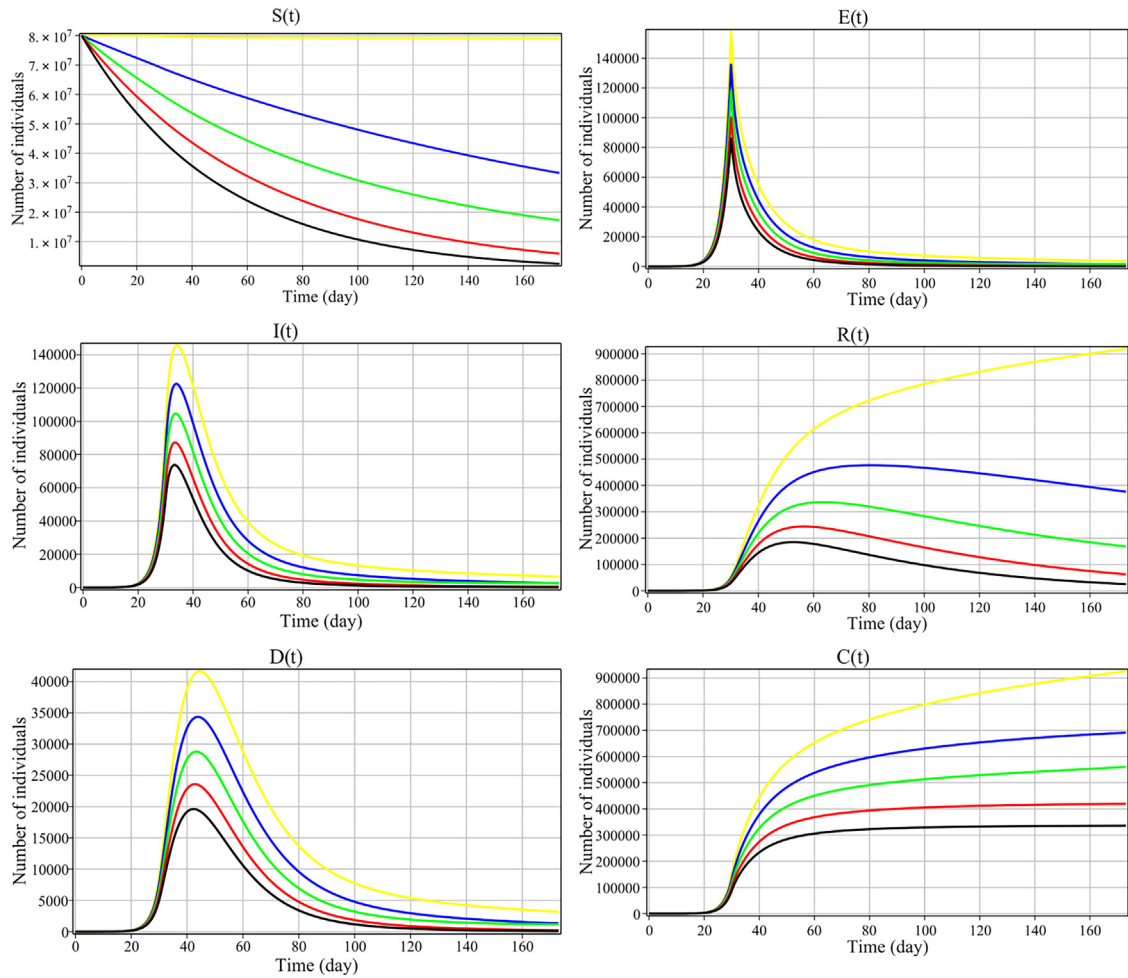
Fig. 9. Sensitivity analysis of the model regarding μ when $\mu = 0$ (yellow solid), $\mu = 0.005$ (blue solid), $\mu = 0.01$ (green solid), $\mu = 0.015$ (red solid), $\mu = 0.02$ (black solid).

of deaths and critical cases $D(t)$ is increasing in the first 45 days after the short of the epidemic. Afterward, this number decreases especially after the end of the quarantine. However, the number of cases $C(t)$ continues to rise. The plot of the quantity $\mathcal{R}_{eff}$ defined by (7) is depicted in Fig. 4. Each infected individual produces more than one new infected case and the virus can be spread through the population (Fig. 4).

Sensitivity analysis

The sensitivity of the COVID-19 model in (1) is investigated concerning the variations of the parameters β_0, α, μ, and κ. For this reason, several scenarios are considered:

First scenario. Let's set $\alpha = 0, \mu = 0.02, \beta_0 = 1.2, \kappa = 1100$ during disease (without governmental action and quarantine). In Fig. 5, the impact of this scenario is observed and it shows that without governmental action and quarantine, the number of infected cases and fatality will increase drastically. Also, a new peak of the disease is observed on the time interval [80, 100] and some mutations are seen in the number of infected and dead.

Second scenario. The functions of model (1) are depicted for $\beta_0 = 0.6, 0.9, 1.2, 1.5, 1.8$ and $\kappa = 1100$ in Fig. 6. The results of this scenario show that by increasing the transmission rate β_0, the number of exposed, infected, removed, and critical people increase. After a decreasing trend, we observe another mutation again over the time interval [100, 140].

Third scenario. The functions of model (1) are plotted for $\alpha = 0.5, 0.6, 0.7, 0.8, 0.9$ and $\kappa = 1100$ in Fig. 7. As observed, the increase of values of the parameter α (governmental action strength) decreases the number of cases and fatality. That shows by increasing the governmental actions and programs to reduce the spread of the virus, such as establishing quarantine, forcing use of masks, and observing the social distances, the number of cases and deaths will decrease and even the number of exposed, infected, and dead people reaches zero.

Forth scenario. Different compartmental variables of model (1) are depicted for various values of $\kappa = 800, 1100, 1400, 1700, 2000$ in Fig. 8. Increasing values of the quantity κ leads to reduce the number of exposed, infected, removed, and dead individuals and cumulative cases significantly. This shows that notwithstanding governmental actions, people should follow health protocols and quarantine in order to control the disease.

Fifth scenario. The compartmental variables of model (1) are plotted for various values of $\mu = 0, 0.005, 0.01, 0.015, 0.02$, and $\kappa = 1100$ in Fig. 9. The increase in the value of the parameter μ results in decreasing the number of cases and fatalities.

Discussion and conclusion

COVID-19 prevalence has appeared as a major issue since 2019 not only in some specific regions but also in the whole world. This work handled to propose a mathematical model involving seven ordinary differential equations for studying the dynamic behaviour of the coronavirus disease 2019 (COVID-19) in Iran. We utilised a conceptual framework derived from the model applied to Wuhan, China Corona cases ([6]). The parameters of the model in [6] were changed with trial and error to coincide with the disease outbreak conditions in Iran. This helps to have a comprehensive understanding of the COVID-19 pandemic in Iran. The existence and uniqueness of the solution of the model were proved. The equilibrium points of the model were determined to investigate the stability of the model. The evaluated basic reproduction number showed that each infected individual can infect more than one individual. A numerical scheme of the Adams-Bashforth family was given for the numerical simulation and investigation of the dynamic behaviour of state variables ($S(t), \mathcal{E}(t), \mathcal{I}(t), \mathcal{R}(t), \mathcal{N}(t), \mathcal{D}(t), C(t)$). Before beginning the quarantine, the number of infected and fatality are more likely to increase due to many social contacts. After quarantine, the number of fatalities and deaths is decreasing with the observance of health protocols. Besides these, the government should also adopt programs to control social contacts, equip hospitals, and provide medicine. To analyse the sensitivity of the model, different strategies were proposed and under adopted initial conditions and strategies, results confirm the importance of decreasing the parameter β_0 and increasing parameters α, κ, and μ. Either decreasing or increasing the related parameters decreases the number of cases in all compartments. Actions such as observing social distancing, the use of the masque, quarantining, increasing the testing of asymptotic cases, and closing airports will reduce the infection rate. Finally, this model could be used as a general proxy for predicting the new cases in the following days/months to prevent more cases in the future in Iran.

Ethics statements

NA.

Declaration of Competing Interest

The authors declare that they have no known competing financial interests or personal relationships that could have appeared to influence the work reported in this paper.

CRediT authorship contribution statement

Khadijeh Sadri: Conceptualization, Methodology, Software, Data curation, Investigation, Writing – original draft, Writing – review & editing. **Hossein Aminikhah:** Investigation, Writing – review & editing, Supervision. **Mahdi Aminikhah:** Conceptualization, Methodology, Data curation, Validation, Investigation, Writing – review & editing.

Data availability

No data was used for the research described in the article.

Acknowledgement

References

[1] S. Oveissi, S.A. Eftekhari, D. Toghraie, Longitudinal vibration and instabilities of carbon nanotubes conveying fluid considering size effects of nanoflow and nanostructure, Physica E 83 (2016) 164–173.

[2] S. Oveissi, D. Toghraie, S.A. Eftekhari, Longitudinal vibration and stability analysis of carbon nanotubes conveying viscous fluid, Physica E 83 (2016) 275–283.

[3] A. Ahmadi Balootaki, A. Karimipour, D. Toghraei, Nano scale lattice Boltzmann method to simulate the mixed convection heat transfer of air in a lid-driven cavity with an endothermic obstacle inside, Physica A 508 (2018) 681–701.

[4] S. Saffari, M. Hashemian, D. Toghraie, Dynamic stability of functionally graded nanobeam based on nonlocal Timoshenko theory considering surface effects, Physica B 520 (2017) 97–105.

[5] WHOCoronavirus Disease (COVID-2019) Situation Reports, WHO, 2022.

[6] Q. Lin, S. Zhao, D. Gao, Y. Lou, S. Yang, S.S. Musa, M.H. Wang, Y. Cai, W. Wang, L. Yang, D He, A conceptual model for the coronavirus disease 2019 (COVID-19) outbreak in Wuhan, China with individual reaction and governmental action, Int. J. Infect. Dis. 93 (2020) 211–216.

[7] B.S.T. Alkahtani, S.S. Alzaid, A novel mathematics model of covid-19 with fractional derivative. Stability and numerical analysis, Chaos. Soliton. Fract. 138 (2020), doi:10.1016/j.chaos.2020.110006.

[8] F. Ndairou, I. Area, J.J. Nieto, D.F.M. Torres, Mathematical modeling of COVID-19 transmission dynamics with a case study of Wuhan, Chaos. Soliton. Fract. 135 (2020), doi:10.1016/j.chaos.2020.109846.

[9] T.M. Chen, J. Rui, Q.P. Wang, J.A. Cui, L Yin, A mathematical model for simulating the phase-based transmissibility of a novel coronavirus, Infect. Dis. Poverty. 9 (24) (2020), doi:10.1186/s40249-020-00640-3.

[10] B.F. Maier, D Brockmann, Effective containment explains subexponential growth in recent confirmed COVID-19 cases in China, Science 368 (6492) (2020) 742–746, doi:10.1126/science.abb4557.

[11] G. Giordano, F. Blanchini, R. Bruno, P. Colaneri, A. Di Filippo, A. Di Matteo, M. Colaneri, Modelling the COVID-19 epidemic and implementation of population-wide interventions in Italy, Nat. Med. 26 (2020) 855–860.

[12] R. Din, A.R. Seadawy, K. Shah, A. Ullah, D Baleanu, Study of global dynamics of COVID-19 via a new mathematical model, Results. Phys. 19 (2020) 103468.

[13] D. Baleanu, H. Mohammadi, S. Rezapour, A fractional differential equation model for the COVID-19 transmission by using the Caputo-Fabrizio derivative, Adv. Differ. Equ-NY. 299 (2020), doi:10.1186/s13662-020-02762-2.

[14] M. Higazy, Novel fractional order SIDARTHE mathematical model of COVID-19 pandemic, Chaos. Soliton. Fract. 138 (2020) 110007.

[15] P. Samui, J. Mondal, S. Khajanchi, A mathematical model for COVID-19 transmission dynamics with a case study of India, Chaos. Soliton. Fract. 140 (2020) 110173.

[16] C. Xu, Y. Yu, Y.Q. Chen, Z. Lu, Forecast analysis of the epidemics trend of COVID-19 in the USA by a generalized fractional-order SEIR model, Nonlinear. Dyn. 101 (2020) 1621–1634.

[17] S. Ghahremanian, M.M. Rashidi, K. Raeisi, D. Toghraie, Molecular dynamics simulation approach for discovering potential inhibitors against SARS-CoV-2: a structural review, J. Mol. Liq. 354 (2022) 118901.

[18] B. Wacker, J. Schlüter, Time-continuous and time-discrete SIR models revisited: theory and applications, Adv. Differ. Eqs. 556 (2020), doi:10.1186/s13662-020-02995-1.

[19] K. Diethelm, The Analysis of Fractional Differential equations: An application-Oriented Exposition Using Differential Operators of Caputo type, Springer Science & Business Media, 2010.

[20] E. Ahmed, A. El-Sayed, H.A. El-Saka, On some Routh-Hurwitz conditions for fractional order differential equations and their applications in Lorenz, Rossler, Chua and Chen systems, Phys. Lett. A. 358 (2006) 1–4.

[21] P. Van den Driesschea, J. Wamough, Reproduction numbers and sub-threshold endemic equilibria for compartmental models of disease transmission, Comput. Math. Biosci. 180 (2002) 29–48.

[22] K. Diethelm, N.J. Ford, A.D. Freed, A predictor-corrector approach for the numerical solution of fractional differential equations, Nonlinear. Dyn. 29 (2002) 3–22.

[23] Y.T. Toh, C. Phang, J.R. Loh, New predictor-corrector scheme for solving nonlinear differential equations with Caputo-Fabrizio operator, Math. Meth. Appl. Sci. 42 (2018) 175–185, doi:10.1002/mma.5331.

[24] J.E. Solis-Perez, J.F. Gomez-Aguilar, A. Atangana, Novel numerical method for solving variable-order fractional differential equations with power, exponential and Mittag-Leffler laws, Chaos. Soliton. Fract. 114 (2018) 175–185.

[25] Y. Liu, X. Yin, L. Feng, H. Sun, Finite difference scheme for simulating a generalized two-dimensional multi-term time fractional non-Newtonian fluid model, Adv. Differ. Equ-NY. 422 (2018) 442.

[26] X. Zhao, X. Hu, W. Cai, G.E. Karniadakis, Adaptive finite element method for fractional differential equations using hierarchical matrices, Comput. Method. Appl. Mech. Eng. 325 (2017) 56–76.